Why do Fish Have a "Fish-Like Geometry"?

Hiroshi Kagemoto
The University of Tokyo,
5-1-5 Kashiwanoha,
Kashiwa City, Chiba 277-8563, Japan
e-mail: kagemoto@k.u-tokyo.ac.jp

Most fish share a common geometry, a streamlined anterior body and a deep caudal fin, connected to each other at a tail-base neck, where the body almost shrinks to a point. This work attempts to explain the reason that fish exhibit this type of geometry. Assuming that the fish-like geometry is a result of evolution over millions of years, or, that bodies of modern-day fish have been optimized in some manner as a result of evolution, this work investigates the optimum geometry for a swimming object through existing mathematical optimization techniques to check whether the result obtained is the same as the naturally observed fish-like geometry. In this analysis, the work done by a swimming object is taken as the objective function of the optimization. It is found that a fish-like geometry is in fact obtained mathematically, provided that the appropriate constraints are imposed on the optimization process, which, in turn, provides some clues that explain the reason that fish have a fish-like geometry. [DOI: 10.1115/1.4025646]

1 Introduction

Almost all species of fish exhibit a characteristic bodily feature, that is, they have a fish-like geometry. In our terms, a fish-like geometry is that composed of a streamlined anterior body and a deep caudal fin that are connected to each other at the tail-base neck where the body almost shrinks to a point. It is also characteristic that a fish undulates its body laterally in a progressing wave mode when it swims. Lighthill [1] showed how a thrust force could be produced by undulating motions using what he refers to as an "elongated-body" theory. Wu [2] obtained the explicit expression of a thrust force composed of two terms, one of which is identical to Lighthill's result and the other of which represents the effect of the vortices shed from the contracting part of a fish body. Recent studies have revealed that fish are exploiting vortices generated by their own motions in thrusting or maneuvering their bodies, while actively manipulating vortices by their tail fin (Wolfgang et al. [3] and Triantafyllou et al. [4]). Vorticity generated by their undulations of the body merges with the vorticity shed at the trailing edge of the tail resulting in a pair of counter-rotating vortices and; hence, thrust jet (Wolfgang et al. [3]). It has also been clarified that proper combination of lateral and angular motions (amplitude, phase, and frequency) of their bodies results in high efficiency of their swimming, which may really be employed by existing fish (Triantafyllou et al. [5]).

The objective of this paper is to answer a self-imposed question: Why do fish have a fish-like geometry? If we believe that the geometry of fish has been optimized over millions of years by evolution for the act of swimming, then it may be reproduced by a computerized optimization process beginning with an arbitrary geometry. This optimization process was previously carried out by Kagemoto et al. [6]. They demonstrated that a fish-like geometry could be reproduced through mathematical means. This present paper is the extension of that previous work.

In this study, assuming the principles of evolution mentioned above, an optimum geometry of a swimming object is determined such that the work done by its muscles while it is swimming is minimized. The swimming object is replaced by an elastic beam of a spatially varying cross section having a spatially varying elastic modulus. With this, the swimming motion is modeled as an oscillation of the elastic beam that undulates laterally with a progressing wave mode under the forces exerted by the ambient flow as well as from the muscles.

Optimization methods used for a swimming object have recently appeared in several papers. Among them, Kern and Koumoutsakos [7] identified the optimum undulation modes of a swimming object using an evolutionary algorithm and accounting for both burst swimming speed and swimming efficiency as objective functions. This previous work showed that the kinematics of burst swimming is characterized by the large amplitude of tail undulations while in efficient swimming, significant lateral undulation occurs along the entire length of the body. The work of Eloy and Schouveiler [8] identified optimal swimming modes in the propulsion performance of a flexible plate undergoing an arbitrary harmonic motion in a two-dimensional, inviscid fluid.

In each of those studies, optimum swimming motions were identified through the optimization process while the fish geometry was given a priori. The work of Tokic and Yue [9], on the other hand, performed a multiobjective optimization for two conflicting locomotive performance measures: maximum sustained swimming speed and minimum cost of transport of a fish, and ultimately identified an optimal shape as well as an optimal undulating swimming motion. In their work, the optimization process also considered physiological feasibility of an identified shape and motion such that only realistic characteristics could be optimized.

In this present study, we identify an optimum geometrical shape of a swimming object by taking the work done by the object as the objective function. Additionally, the spatial variation of the elastic modulus along the object and the phase speed of the undulating motion are also included as the design parameters.

2 Optimization of a Swimming Object

2.1 Equation of Motion and the Work Done by a Fish. We assume that fish have evolved into ingenious swimmers and can proceed through a fluid, encumbered, while performing the least amount work. In order to examine the work done by a swimming object, we model the body of the swimming object as an elastic beam with both variable cross-sectional geometry and elastic modulus E. The equation of the motion of the swimming object may be written as follows:

$$\rho S \frac{\partial^2 h}{\partial t^2} + \frac{\partial^2}{\partial x^2}\left(EI \frac{\partial^2 h}{\partial x^2}\right) = F(x,t) \tag{1}$$

Contributed by the Fluids Engineering Division of ASME for publication in the JOURNAL OF FLUIDS ENGINEERING. Manuscript received September 18, 2012; final manuscript received August 1, 2013; published online November 6, 2013. Assoc. Editor: Zhongquan Charlie Zheng.

$h(x, t)$: lateral displacement, $S(x)$: cross-sectional area, $E(x)I(x)$: bending rigidity, and $\rho(x)$: mass density.

Here $F(x, t)$ represents the external force, which is assumed to be decomposed into the following two parts:

$$F(x,t) = F_1 + F_2 \tag{2}$$

where F_1 and F_2 represent the force exerted by muscles and the force exerted by ambient fluids, respectively.

According to Lighthill [1], we suppose F_2 can be expressed in the following form:

$$F_2(x,t) = -\left(\frac{\partial}{\partial t} + U\frac{\partial}{\partial x}\right)\left[\left(\frac{\partial h}{\partial t} + U\frac{\partial h}{\partial x}\right)\rho_w A(x)\right] \tag{3}$$

U represents the fish's swimming speed and $\rho_w A(x)$ represents the local added mass associated with the object's lateral motion $h(x, t)$. Using the above decomposition, the equation of motion is rewritten as follows:

$$\rho S\frac{\partial^2 h}{\partial t^2} + \frac{\partial^2}{\partial x^2}\left(EI\frac{\partial^2 h}{\partial x^2}\right) + \left(\frac{\partial}{\partial t} + U\frac{\partial}{\partial x}\right)\left[\left(\frac{\partial h}{\partial t} + U\frac{\partial h}{\partial x}\right)\rho_w A(x)\right] = F_1(x,t) \tag{4}$$

The mean work W done by the fish's muscles in one period T of the undulating motion is written

$$W = \frac{1}{T}\int_0^T \int_0^\ell F_1(x,t)\cdot\frac{\partial h}{\partial t}dxdt \tag{5}$$

where ℓ denotes the fish's length.

Here, we further assume that the objective function that should be minimized is W', which is defined in the following form, rather than W:

$$W' \equiv \frac{1}{T}\int_0^T \int_0^\ell \left|F_1(x,t)\cdot\frac{\partial h}{\partial t}\right|dxdt \tag{6}$$

Although the validity of the usage of W' instead of W is not obvious, the definition of W' accounts for the fact of the mechanical systems of living creatures that their muscles cannot extract energy back from negative work.

2.2 Optimization of a Swimming Object. In this section, we identify the optimum configuration of a swimming object that minimizes the objective function W', given by Eq. (6). Among various existing optimization techniques, one of the nonlinear programming techniques [11, 12] is used in the present study.

2.2.1 Description of the Problem. Substituting $F_1(x, t)$ given by Eq. (4) into Eq. (6), we minimize the following objective function Γ:

$$\Gamma \equiv \frac{1}{T}\int_0^T \int_0^\ell \left|\left\{\rho S\frac{\partial^2 h}{\partial t^2} + \frac{\partial^2}{\partial x^2}\left(EI\frac{\partial^2 h}{\partial x^2}\right) + \left(\frac{\partial}{\partial t} + U\frac{\partial}{\partial x}\right)\left[\left(\frac{\partial h}{\partial t} + U\frac{\partial h}{\partial x}\right)\rho_w A(x)\right]\right\}\frac{\partial h}{\partial t}\right|dxdt \tag{7}$$

under the following constraints.

Thrust = drag. The mean thrust force (T) should exactly counteract the mean drag force (D) so that the fish can swim with a constant averaged speed. If we follow Lighthill's elongated body theory [1], T can be expressed in the following form:

$$T = \frac{1}{2}\rho_w A(\ell)\left\{\overline{\left(\frac{\partial h}{\partial t}\right)^2} - U^2\overline{\left(\frac{\partial h}{\partial x}\right)^2}\right\}_{x=\ell} \tag{8}$$

Here, the overbar indicates that the mean value in time is to be taken.

As for the drag force, we assume it can be written as follows:

$$D = \frac{1}{2}\rho_w S_f U^2\cdot C_f \tag{9}$$

$\rho_w A(\ell), S_f, C_f$ represent the added mass of the tail-end section (at $x = \ell$), the surface area of the object, and the drag coefficient, respectively.

The Lighthill's elongated-body theory [1], which was adapted in the present study, assumes steadily translating body and its wake. The theory is relatively simple but thrust forces predicted by the theory agrees fairly well with those predicted by a more rigorous vortex-lattice flow model, as observed in, e.g., Kagemoto et al. [10], although the vortex-lattice theory also assumes that the wake profile remains to be the same and translates with the same speed as that of the swimming body. It is indicated that a wake structure of even a steadily swimming body is essentially unsteady and quite complex (e.g., Wolfgang et al. [3]). Therefore, it may be desirable to account for the effect of the unsteadiness on the hydrodynamic forces acting on a swimming body, but, as shown in Kagemoto et al. [10], experimental results of the thrust forces produced by a steadily swimming body turned out to be explained fairly well by the vortex-lattice theory. These facts may justify the fact that the present work used the Lighthill's theory [1] for the prediction of thrust forces induced by a steadily swimming body.

The total volume (∇) should at least have a certain value (V_c). It may be reasonable to assume that a fish should have certain amount of volume V_c that contains all of its necessary physiological matter. (From the sole viewpoint of the minimization of work, it is apparent that a smaller volume is better.)

The maximum depth (d_{max}) of the anterior region of the swimming object is equal to the tail-end depth ($d_{x=\ell}$). Although this constraint may seem to be intentional to obtain a fish-like geometry, it is imposed as a constraint in order to avoid the geometry in which most of the mass is concentrated around the head where lateral motion is small, which is an unrealistic configuration from the physiological point of view.

No recoils. The following quantities are called recoils (Lighthill [1]) and should be as small as possible, R_1, R_2. Recoils physically represent the force and the angular moment that the corresponding swimming object suffers as rigid-body motions in order to compensate for the difference between the hydrodynamic force/moment and the mass inertia force/moment associated with the lateral motions h,

$$R_1 \equiv \int_0^\ell \rho S(x)\frac{\partial^2 h}{\partial t^2}dx + \int_0^\ell \rho_w\left(\frac{\partial}{\partial t} + U\frac{\partial}{\partial x}\right)\left\{A(x)\left(\frac{\partial h}{\partial t} + U\frac{\partial h}{\partial x}\right)\right\}dx \tag{10}$$

$$R_2 \equiv \int_0^\ell x\rho S(x)\frac{\partial^2 h}{\partial t^2}dx + \int_0^\ell x\rho_w\left(\frac{\partial}{\partial t} + U\frac{\partial}{\partial x}\right)\left\{A(x)\left(\frac{\partial h}{\partial t} + U\frac{\partial h}{\partial x}\right)\right\}dx \tag{11}$$

This constraint was imposed because large recoils should be uncomfortable for fish as well as because large recoils of fish are not observed in nature.

Other than these constraints, we suppose that the lateral displacement $h(x, t)$ of a swimming object is expressed in the following form:

$$h = a\left(\frac{x}{\ell} - \frac{x_0}{\ell}\right)^2\cos(kx - \omega t) \tag{12}$$

k: wave number $2\pi/\lambda$, where λ is the wavelength of the body undulation, and ω: angular frequency of the body undulation.

An example of the undulating motion of the swimming object given by the above mathematical form is depicted in Fig. 1. The curves shown in the figure are the instantaneous geometries of the swimming object at $t=0$, $T/4$, $T/2$, $3T/4$, where T represents the period of the undulating motion, when the parameters in Eq. (12) are assumed to be as follows:

$$x_0 = 0.3, \quad k = 2\pi, \quad \omega/k = 5.5, \quad a = 1/7$$

x_0 in Eq. (12) represents the pivoting point where the displacement is always zero. Equation (12) can be considered to represent the so-called carangiform motion, in which the fish's lateral undulating motion is mostly confined to the posterior part of the fish.

We allow the following three design variables to vary in the optimization process:

(1) the local depth of a swimming object, $d(x)$.
(2) the local elastic modulus of a swimming object, $E(x)$.
(3) the ratio of the phase speed c of the lateral undulating motion to the swimming speed U, hereafter denoted as γ.

The phase speed c of the lateral undulating motion is related to k, ω of Eq. (12) as

$$c = \frac{\omega}{k} \tag{13}$$

We express the volume ∇, surface area S_f of the swimming object, second moment of area of the local cross section $I(x)$, and the added mass $\rho_w A(x)$ in terms of the three design variables, as follows:

$$\nabla = \int_0^\ell \beta d^2(x)dx \tag{14}$$

$$S_f = 2\int_0^\ell d(x)dx \tag{15}$$

$$I(x) = \frac{1}{12}(\beta d)^{3}\cdot d(x) \tag{16}$$

$$\rho_w A(x) \approx \frac{\pi}{4}\rho_w d^2(x) \tag{17}$$

Here, it is assumed that the local cross section is approximated by a rectangle of depth $d(x)$ and width $\beta \cdot d(x)$, where β is assumed to be of constant value (in the present analysis, $\beta = 0.1$ is used).

Using Eqs. (12), (15), and (17), the mean thrust force T and the drag force D are, respectively, rewritten, as follows:

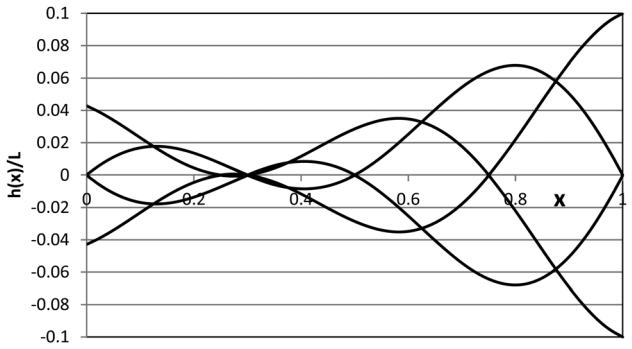

Fig. 1 The assumed instantaneous lateral displacement of a swimming object

$$T = \frac{\pi}{16}\rho_w d^2(\ell)U^2 \times \left[(ak)^2\{1-(x_0/\ell)\}^4(\gamma^2-1) - 4(a/\ell)^2\{1-(x_0/\ell)\}^2\right] \tag{18}$$

$$D = \rho_w \int_0^\ell d(x)dx \cdot U^2 \cdot C_f \tag{19}$$

We express the square of the local depth $d^2(x)$ and the local elastic modulus $E(x)$ by the following simple polynomials:

$$d^2(x) = \sum_{m=1}^{M} a_m x^m, \quad E(x) = \sum_{m=0}^{M-1} b_m x^m \tag{20}$$

The polynomial for $d^2(x)$ begins with $m=1$ instead of $m=0$ so that the depth of the head ($x=0$) is always zero, in other words, it is assumed that the swimming object is point-nosed.

For the present analysis, $M=10$ was used.

By making use of one of the existing nonlinear programming techniques [11, 12], the minimization of the objective function Γ (Eq. (7)) under the four constraints mentioned above can be transformed into the minimization of a new objective function Γ', with no constraints. In the present case, the new objective function Γ' that should be minimized is written as follows:

$$\begin{aligned}\Gamma' = \Gamma &+ \frac{1}{\varepsilon_1}\left[\int_0^T \left|\int_0^\ell \rho S(x)\frac{\partial^2 h}{\partial t^2}dx \right.\right. \\ &\left.\left. + \int_0^\ell \left(\frac{\partial}{\partial t} + U\frac{\partial}{\partial x}\right)\left\{\rho_w A(x)\left(\frac{\partial h}{\partial t} + U\frac{\partial h}{\partial x}\right)\right\}dx\right| dt\right] \\ &+ \frac{1}{\varepsilon_2}\left[\int_0^T \left|\int_0^\ell x\rho S(x)\frac{\partial^2 h}{\partial t^2}dx \right.\right. \\ &\left.\left. + \int_0^\ell x\left(\frac{\partial}{\partial t} + U\frac{\partial}{\partial x}\right)\left\{\rho_w A(x)\left(\frac{\partial h}{\partial t} + U\frac{\partial h}{\partial x}\right)\right\}dx\right| dt\right] \\ &+ \left\{\frac{1}{\varepsilon_3}(T-D)\right\}^2 \\ &+ \frac{1}{\varepsilon_4}\{|\nabla - V_c| - (\nabla - V_c)\} \\ &+ \left\{\frac{1}{\varepsilon_5}(d_{\max} - d(\ell))\right\}^2 \\ &+ \frac{1}{\varepsilon_6}\int_0^\ell \{|d(x)| - d(x)\}dx \\ &+ \frac{1}{\varepsilon_7}\int_0^\ell \{|E(x)| - E(x)\}dx \\ &+ \frac{1}{\varepsilon_8}(|\gamma| - \gamma)\end{aligned} \tag{21}$$

$\varepsilon_1, \varepsilon_2, \ldots$ are certain small positive numbers that are added so that each term in Eq. (21) becomes more or less of the same order.

The last three terms are added to ensure that positive $d(x), E(x), \gamma$ are obtained.

The fourth term accounts for the constraint $T=D$, since, as thrust force (T) deviates from the drag force (D), the term becomes disproportionately large, the requirement of minimization of Γ' imposes the thrust force T to be around the drag force D. Similarly, the fifth and sixth terms account for the second and third constraints, respectively. The second and third terms ensure that the constraints associated with the recoils are satisfied.

For ε, the following values were used in the present study:

$$\begin{aligned}
\varepsilon_1 &= \rho_w V_c g \cdot \overline{T} \times 0.1 \\
\varepsilon_2 &= \rho_w V_c g \cdot \overline{T} \cdot \frac{\ell}{2} \times 0.1 \\
\varepsilon_3 &= \frac{1}{2}\rho_w \overline{S_f} C_f U^2 \times 0.05 \\
\varepsilon_4 &= V_c \times 0.05 \\
\varepsilon_5 &= \overline{d} \times 10^{-4} \\
\varepsilon_6 &= \overline{d} \cdot \ell \times 10^{-3} \\
\varepsilon_7 &= \overline{E} \cdot \ell \times 10^{-4} \\
\varepsilon_8 &= 10^{-8}
\end{aligned} \tag{22}$$

The values with the overbars are certain standard values given as follows:

$$\begin{aligned}
\overline{d} &\equiv \sqrt{V_c/\beta\ell} \\
\overline{S_f} &\equiv V_c/\frac{1}{4}\beta\ell \\
\overline{E} &\equiv \omega^2\left(\rho\overline{S} + \rho_w\overline{A}\right)/\frac{1}{12}\beta^3\overline{d}^4k^4 \\
\overline{S} &\equiv \beta \cdot \overline{d}^2 \\
\overline{A} &\equiv \frac{\pi}{4}\overline{d}^2
\end{aligned}$$

2.2.2 Parameters. In order to identify the optimum $d(x), E(x)$, and γ, we need to choose appropriate values for several parameters. First, we assume that the Strouhal number S_t, which is defined as follows, is always 0.30,

$$S_t \equiv \frac{f \cdot 2A_m}{U} \tag{23}$$

where $f \cdot 2A_m$ represents product of the frequency and the double amplitude of the tail-end motion. The value of 0.30 is derived from the stability analysis of a fish's wake (Triantafyllou et al. [13]). Other than the stability analysis, in Triantafyllou et al. [5] empirical values of the Strouhal number obtained from the observations of real fish are summarized, all of which are distributed around 0.30 regardless of swimming speed, tail-beat frequency, and body length.

The values of the other parameters used for the present analysis are

$$\begin{aligned}
V_C &= 0.015\ell^3 \\
x_0/\ell &= 0.3 \\
C_f &= 0.004 \\
A_m &= 0.1 \cdot \ell \\
U &= 10\ell, 5\ell, 2\ell \text{ per unit time}
\end{aligned} \tag{24}$$

If we follow the Schoenherr line, the above skin-friction drag coefficient C_f corresponds a Reynolds number of $\sim 10^6$.

As for the swimming speeds, we can observe from the data in Table 1 of Ref. [14] (Bainbridge) that the swimming speeds of fish are distributed over $U = 2\ell \sim 10\ell$ per second, and therefore, $U = 2\ell, 5\ell$, and 10ℓ are chosen as representative speeds, with $\ell = 1.0$m.

From Eq. (23), only two of the three parameters from among U, A_m, f can be independently chosen. From the values of A_m, U specified above, the tail-beat frequencies f are determined as $f = 15$Hz, 7.5Hz, 3Hz, respectively, corresponding to $U = 10\ell$, 5ℓ, 2ℓ. Bainbridge [14] presented the laboratory observed relationships between the fish's speed U and the frequency f of the tail-beat. From the observation facts presented in the paper, it can be known that, regardless of the species of fish and swimming speeds, the speed (U) is approximately related to the frequency (f) by the following formula:

$$\frac{U}{\ell} \approx \frac{3}{4}f \tag{25}$$

Substitution of Eq. (25) into Eq. (23) gives

$$A_m = 0.1125 \cdot \ell \tag{26}$$

which justifies the assumed amplitude A_m of the tail specified in Eq. (24). (Triantafyllou et al. [5] refers to the results of Payatetskiy [15] obtained from the observations of three Black Sea species saying that the same linear relationship between U/ℓ and f holds with the proportional coefficient 1/1.39 (against 1/1.33 in the case of Eq. (25)) and the amplitude/length ratio $A_m/\ell = 0.10 - 0.12$ for all the three species regardless of their body length.

2.3 Results and Discussion

2.3.1 Optimum Shape. Figure 2 shows the configuration identified as optimum when $U = 5\ell$. The horizontal axis of the figure represents the x coordinate (head: $x = 0$, tail: $x = 1$). Although the tail-base neck is not as distinct as that of a fish, the identified shape is similar in appearance to a fish. If compared the present optimal shape (mass = ~20 kg, swimming speed = 2–10 m/s) with those shown in Fig. 4 of Tokic and Yue [9], they are similar to each other in that both of them exhibit a streamed-line anterior body connected via tail-base neck with a posterior body possessing a significant depth at its end.

Figure 3 shows the minimization of the objective function in the optimization process, which may validate the correctness of the result shown in Fig. 2 in that the value of the objective function given by Eq. (21) is reduced to a very small value. While useful, this result does not necessarily guarantee that the identified value is a global minimum.

Figure 4 compares the optimum shape of the swimming object identified for different swimming speeds $U = 2\ell, 5\ell$, and 10ℓ. It is

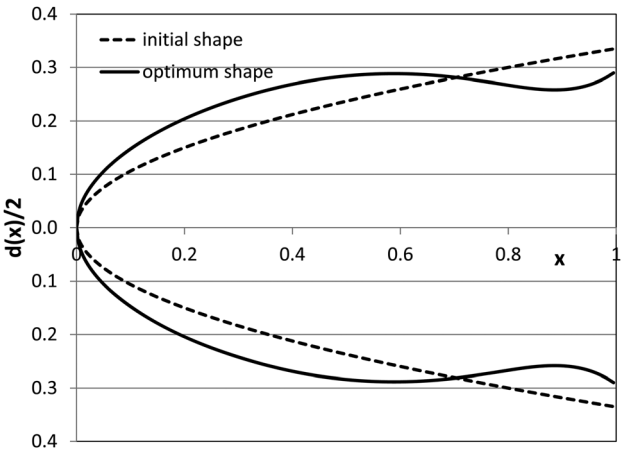

Fig. 2 Optimum shape of an object swimming with $U = 5\ell$

Table 1 Optimum value of γ

	$U = 2\ell$	$U = 5\ell$	$U = 10\ell$
γ	1.0684	1.0687	1.0705

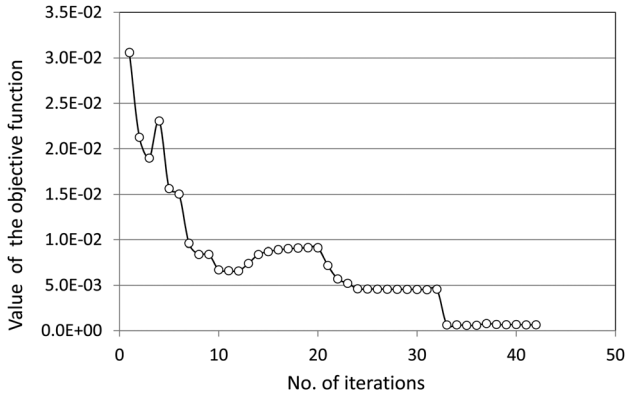

Fig. 3 Reduction of an objective function in the optimization process

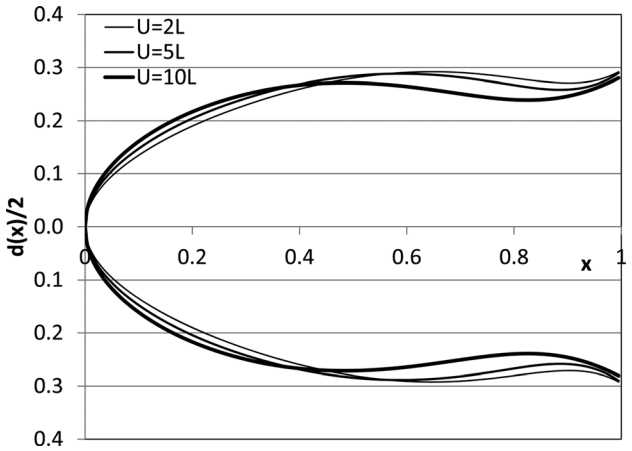

Fig. 4 Comparison of the optimum shapes identified for $U = 2\ell, 5\ell, 10\ell$

observed that the optimum shape is almost the same regardless of the swimming speed.

2.3.2 Optimum Elastic Modulus. Figure 5 compares the optimum lengthwise distribution of the elastic modulus $E(x)$ for different swimming speeds, $U = 2\ell, 5\ell$, and 10ℓ. The unit of the vertical axis is N/m^2.

According to the results shown in the figure, the optimum lengthwise distribution of the elastic modulus $E(x)$ decreases from head to tail. This is seemingly the case even when the swimming

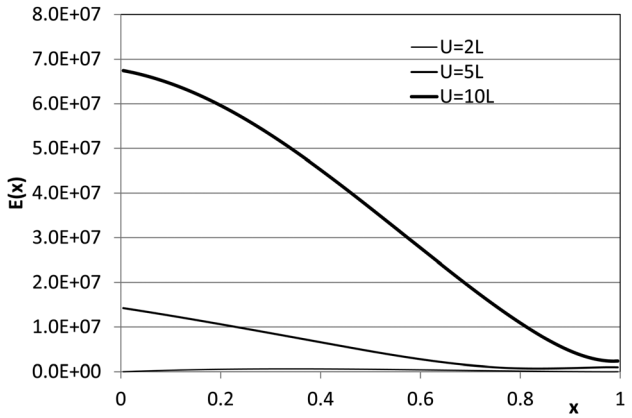

Fig. 5 Comparison of optimum elastic modulus distribution identified for $U = 2\ell, 5\ell, 10\ell$

speed is changed, although the optimum value of the elastic modulus is susceptible to swimming speed as observed in the results shown in Fig. 5, as the modulus becomes minimum just before the tail end and then increases slightly after it. As an elucidating exercise, it may be fortuitous to compare the identified E with those of other materials (for example, steel: $2.0 \times 10^{10}(\mathrm{N/m^2})$ or nylon: $2.0 \times 10^{8}(\mathrm{N/m^2})$, polyethylene: $1.2 \times 10^{7}(\mathrm{N/m^2})$, or rubber: $1.0 \times 10^{5}(\mathrm{N/m^2})$).

Quantitatively, the overall value of the optimum elastic modulus shown in Fig. 5 decreases roughly in proportion to the square of the swimming speed, which may be justified as follows.

The integrand of the objective function (Eq. (7)) is written as

$$\begin{aligned}\left|F_1 \cdot \frac{\partial h}{\partial t}\right| &= \left|\left[\rho S \frac{\partial^2 h}{\partial t^2} + \frac{\partial^2}{\partial x^2}\left(EI\frac{\partial^2 h}{\partial x^2}\right) + \left(\frac{\partial}{\partial t} + U\frac{\partial}{\partial x}\right)\left\{\left(\frac{\partial h}{\partial t} + U\frac{\partial h}{\partial x}\right)\rho_w A\right\}\right] \cdot \frac{\partial h}{\partial t}\right| \\ &\sim \left|\left[(\rho S + \rho_w A)\frac{\partial^2 h}{\partial t^2} + EI\frac{\partial^4 h}{\partial x^4} + 2U\frac{\partial^2 h}{\partial x \partial t}\rho_w A + U^2\frac{\partial^2 h}{\partial x^2}\rho_w A\right] \cdot \frac{\partial h}{\partial t}\right| \end{aligned} \tag{27}$$

When the spatial change of $EI(x)$ is slow, the lower approximation in Eq. (27) is valid.

If the lateral displacement is written as $h(x,t) = h_0 \cdot \cos(kx - \omega t)$, which is approximately the case in the present study,

$$F_1 \cdot \frac{\partial h}{\partial t} \sim -\omega^2\left\{\rho S + \rho_w A\left(1 + \frac{1}{\gamma}\right)^2\right\} + EIk^4 \tag{28}$$

then we know the integrand, and therefore, the objective function has the minimum value when the following relationship is satisfied:

$$EIk^4 = \omega^2\left\{\rho S + \rho_w A\left(1 + \frac{1}{\gamma}\right)^2\right\} \tag{29}$$

Since the amplitude of the tail-end motion A_m and the Strouhal number S_t are not changed with speed, then, from Eq. (23), f/U, and therefore, ω/U should also be of the same value for all speeds.

If $\gamma(= c/U)$ remains unchanged for all speeds, $k(= \omega/\gamma U)$ is also unchanged with all speeds because it is constant. Thus, it may be concluded that EI should be proportional to ω^2(or U^2) in order to minimize the integrand. This partly explains why the optimum value of the elastic modulus $E(x)$ decreases in proportion to U^2 as the swimming speed decreases.

2.3.3 Optimum Undulating Motion. The optimum value of γ identified varies very slightly with speed, as shown by the data in Table 1. This fact confirms Lighthill's argument [1] that good efficiency and substantial thrust are obtained when c is close to but slightly larger than U, meaning that γ is close to but slightly higher than unity.

Table 2 lists the corresponding optimum values of λ (wavelength of undulating motion). We can observe that the wavelength of the optimum undulating motion is independent of the swimming speed.

Table 2 Optimum value of λ

	$U = 2\ell$	$U = 5\ell$	$U = 10\ell$
λ/ℓ	0.712	0.712	0.713

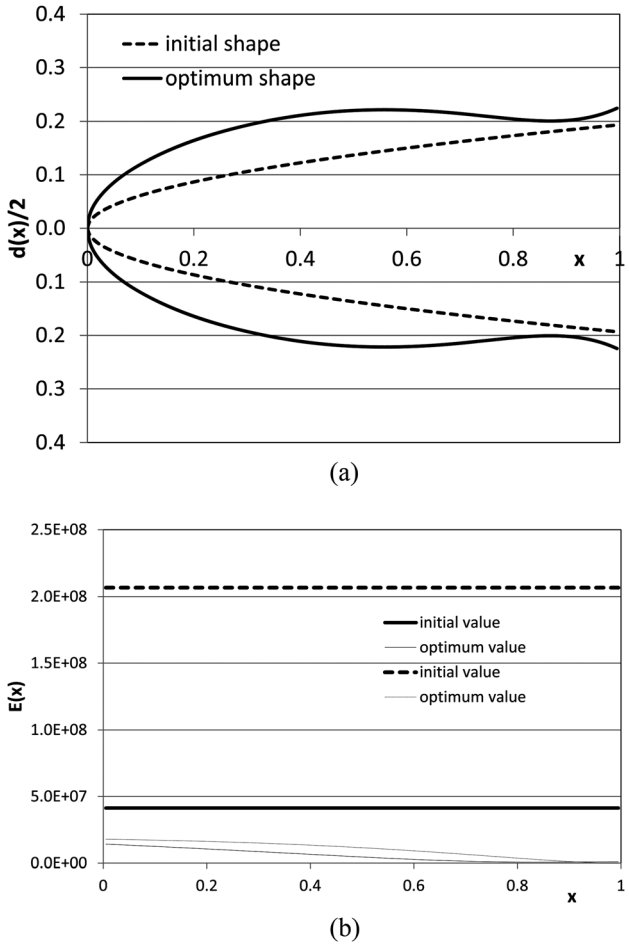

Fig. 6 (*a*) Optimum shape identified starting from a different initial condition ($U = 5\ell$); (*b*) optimum elastic modulus identified starting from a different initial condition ($U = 5\ell$)

When the drag coefficient C_f does not change with speed, then from Eq. (19), the drag force D acting on a fish should be proportional to U^2 which, in turn, implies that the thrust force T should be proportional to U^2. On the other hand, ω/U should also be the same value for all speeds, as described above. Then, since the mean thrust force T in Eq. (18) is rewritten as

$$T = \frac{\pi}{16}\rho_w d^2(\ell)\left(\frac{A}{\ell}\right)^2 U^2\left\{\left(\frac{\omega\ell}{U}\right)^2\left(1-\frac{x_0}{\ell}\right)^2\left(1-\frac{1}{\gamma^2}\right)-4\right\} \tag{30}$$

we can conclude that $1-\frac{1}{\gamma^2}$ remains unchanged with speed, and thus, γ remains unchanged with speed.

2.3.4 Sensitivity to Initial Conditions. Figure 6(*a*) shows the optimum shape for $U = 5\ell$, starting from a different initial shape than that shown in Fig. 2. The final result is similar to but not exactly the same as that shown in Fig. 2. As for the optimum elastic modulus, Fig. 6(*b*) shows the optimum lengthwise distribution of the elastic modulus for $U = 5\ell$, starting from different initial distributions. Again, the final results are similar to each other but not exactly the same.

In optimization problems, it often becomes problematic when the identified result is undetermined, as to whether it is a global minimum or a local minimum. Since in the present study, as many as 21 design variables were involved, it was difficult to ensure that the global minimum was always obtained. It is, however, observed in Figs. 6(*a*) and 6(*b*) that, at least qualitatively, similar results were obtained, although they were not quantitatively identical. The results presented in this paper should be interpreted as qualitative tendencies of a swimming object, though not necessarily the most optimum tendencies.

2.3.5 Effect of Additional Vortex Shedding. Wu [2] showed that the mean thrust produced by a slender fish is given as

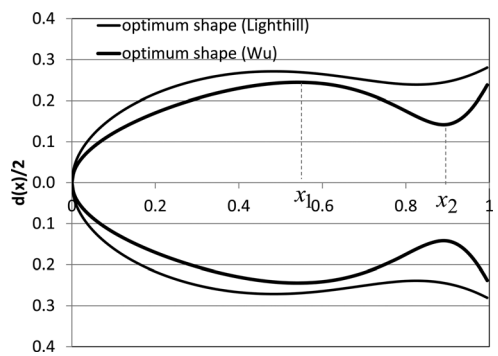

Fig. 7 Comparison of the optimum shape identified while taking the vortex shedding from the edge of the body into consideration (Wu) with that identified while neglecting the vortex shedding from the edge of the body (Lighthill) ($U = 10\ell$)

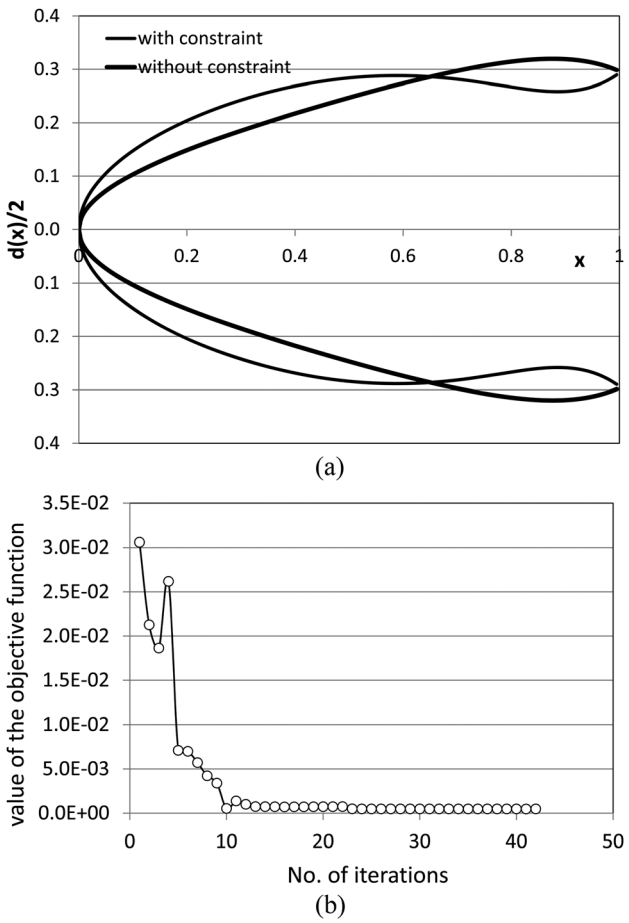

Fig. 8 (*a*) Effect of the constraint on recoils; (*b*) reduction of the objective function in the optimization process

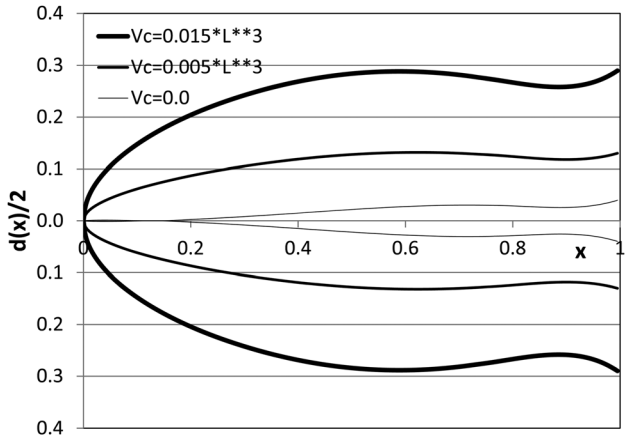

Fig. 9 Effect of the constraint on minimum volume

$$T = \frac{1}{2}\rho A(\ell)\left[\left(\frac{\partial h}{\partial t}\right)^2 - U^2\left(\frac{\partial h}{\partial x}\right)^2\right]_{x=\ell} - \frac{1}{2}\rho\int_{x_1}^{x_2}\overline{\left\{\left(\frac{\partial h}{\partial t}\right)^2 - U^2\left(\frac{\partial h}{\partial x}\right)^2\right\}}\frac{dA}{dx}dx \tag{31}$$

By comparing this with Eq. (8), the first term in Eq. (21) is found to be exactly the same as that given by Lighthill's elongated-body theory [1], while the second term is newly introduced. The second term corresponds to the thrust production due to the vortex sheet shed from the edge of the body between $x = x_1$ (the maximum depth point) to $x = x_2$ (tail-base neck, see Fig. 7).

Figure 7 compares the optimum shape identified by making use of Eq. (31) instead of Eq. (8) for the thrust estimation when the swimming speed is $U = 10\ell$. Although the overall optimum configuration is not changed much due to the consideration of the vortex shedding from the edge of the body, the tail-base neck tends to become more distinct when the vortex shedding from the edge of the body is taken into account. This may be because of the dA/dx term that appears in the second term of Eq. (31), which represents the rate of variation of the added mass in the x direction, and is larger for steeper constriction toward the tail-base neck, thereby contributing a larger thrust force. (In Wolfgang et al. [3], it is said that together with the vorticity shed at the trailing edge of the tail, vorticity is also generated well upstream of the tail by the undulations of the body, which may support the Wu's model [2].)

2.3.6 Effect of Constraints. Figure 8(*a*) shows how the constraint associated with recoils affect the final result. As is observed in the figure, the tail-base neck completely disappears when the constraint on recoils is not imposed. As indicated by Lighthill [1], this implies that a fish's body is shrunk to a tail-base neck in order to avoid excessive recoils, because at this point, the lateral undulating motion is large in carangiform motions.

It could be considered that if having minimal recoil is beneficiary from the aspect of minimal work then a tail-base neck would result even without imposing the constraint associated with recoils. However, as is observed in Fig. 8(*b*), which shows how the objective function is minimized in the optimization process when the constraint on recoils is removed, the objective function (work done by the swimming object) could be very small even without the shrinking at the tail-base neck.

Figure 9 shows how the constraint on the minimum volume, V_c affects the final results. As expected, the volume of the identified optimum swimming object decreases as V_c is reduced.

3 Conclusions

In order to answer the question as to why fish have a fish-like geometry, an optimum geometry of a swimming object was identified by employing as the objective function the work done by the swimming object. The obtained geometry is similar to that of a fish and possesses a tail-base neck.

As a result of the present study, it may be concluded that fish have a fish-like geometry, consisting of a streamlined anterior body in order to reduce the drag force, a caudal fin of large depth in order to attain necessary thrust force, and a tail-base neck in order to reduce excessive recoils.

Along with the optimum geometry, optimum lengthwise distribution of the elastic modulus and optimum phase speed of the lateral undulating motion of a swimming object were identified. Accounting for the spatial variation of the rigidity along the swimming object in the present formulation affects the power needed for fish's muscles significantly.

The obtained results at least qualitatively emulate those of a fish.

Acknowledgment

Most of the present work was conducted while the author was on leave at Massachusetts Institute of Technology (MIT). Valuable comments given by Professor Yue and Professor Triantafyllou of MIT are greatly appreciated.

References

[1] Lighthill, M. J., 1960, "Note on the Swimming of Slender Fish," J. Fluid Mech., **9**, pp. 305–317.
[2] Yao-Tsu Wu, T., 1971, "Hydromechanics of Swimming Propulsion, Part 3. Swimming and Optimum Movements of Slender Fish With Side Fins," J. Fluid Mech., **46**, part 3, pp. 545–568.
[3] Wolfgang, M. J., Anderson, J. M., Grosenbaugh, M. A., Yue, D. K. P., and Triantafyllou, M. S., 1999, "Near-Body Flow Dynamics in Swimming Fish," J. Exp. Biol., **202**, pp. 2303–2327. Available at: http://jeb.biologists.org/content/202/17/2303.long
[4] Triantafyllou, M. S., Triantafyllou, G. S., and Yue, D. K. P., 2000, "Hydrodynamics of Fishlike Swimming," Annu. Rev. Fluid Mech., **32**, pp. 33–53.
[5] Triantafyllou, G. S., Triantafyllou, M. S., and Grosenbaugh, M. A., 1993, "Optimal Thrust Development in Oscillating Foils With Application to Fish Propulsion," J. Fluids Struct., **7**, pp. 205–224.
[6] Kagemoto, H., Yue, D. K. P., and Triantafyllou, M. S., 1997, "Optimization of a Fish-Like Swimming Body," Bull. Am. Phys. Soc., **42**, p. 5533.
[7] Kern S., and Koumoutsakos, P., 2006, "Simulations of Optimized Anguilliform Swimming," J. Exp. Biol., **209**, pp. 4841–4857.
[8] Eloy, C., and Schouveiler, L., 2011, "Optimization of Two-Dimensional Undulatory Swimming at High Reynolds Number," Int. J. Non-linear Mech., **46**, pp. 568–576.
[9] Tokic, G., and Yue, D. K. P., 2012, "Optimal Shape and Motion of Undulatory Swimming Organisms," Proc. R. Soc. B, **279**, pp. 3065–3074.
[10] Kagemoto, H., Wolfgang, M. J., Yue, D. K. P., and Triantafyllou, M. S., 2000, "Force and Power Estimation in Fish-Like Locomotion Using a Vortex-Lattice Method," ASME J. Fluids Eng., **122**, pp. 239–253.
[11] Kowalik, J., and Osborne, M. R., 1968, *Methods for Unconstrained Optimization Problems*, American Elsevier Publishing Company, New York.
[12] Fiacco, A., and McCormick, G. P., 1968, *Nonlinear Programming Sequential Unconstrained Minimization Techniques*, John Wiley & Sons, New York.
[13] Triantafyllou, G. S., Triantafyllou, M. S., and Chryssostomidis, C. C., 1986, "On the Formation of Vortex Streets Behind Stationary Cylinders," J. Fluid Mech., **170**, pp. 461–477.
[14] Bainbridge, R., 1957, "The Speed of Swimming Fish as Related to Size and to the Frequency and Amplitude of the Tail Beat," J. Exp. Biol., **35**, pp. 109–133. Available at: http://jeb.biologists.org/content/35/1/109.full.pdf+html
[15] Pyatetskiy, V. E., 1971, "Kinematic Swimming Characteristics of Some Fast Marine Fish," *Hydrodynamic Problems of Bionics*, G. V. Logvinovich, ed., Joint Publications Research Service, Washington, DC, pp. 12–23.